

Note: A simple image processing based fiducial auto-alignment method for sample registration

Wesley D. Robertson, Lucas R. Porto, Candice J. X. Ip, Megan K. T. Nantel, Friedjof Tellkamp, Yinfei Lu, and R. J. Dwayne Miller

Citation: Review of Scientific Instruments 86, 086105 (2015); doi: 10.1063/1.4929408

View online: http://dx.doi.org/10.1063/1.4929408

View Table of Contents: http://scitation.aip.org/content/aip/journal/rsi/86/8?ver=pdfcov

Published by the AIP Publishing

Articles you may be interested in

Simultaneous 3D–2D image registration and C-arm calibration: Application to endovascular image-guided interventions

Med. Phys. 42, 6433 (2015); 10.1118/1.4932626

Validation of a deformable image registration technique for cone beam CT-based dose verification Med. Phys. **42**, 196 (2015); 10.1118/1.4903292

A three-dimensional head-and-neck phantom for validation of multimodality deformable image registration for adaptive radiotherapy

Med. Phys. 41, 121709 (2014); 10.1118/1.4901523

Robust methods for automatic image-to-world registration in cone-beam CT interventional guidance Med. Phys. **39**, 6484 (2012); 10.1118/1.4754589

Influence of imaging source and panel position uncertainties on the accuracy of 2D/3D image registration of cranial images

Med. Phys. 39, 5547 (2012); 10.1118/1.4742866

Excellence in Science Powerful, Multi-functional UV-Vis-NIR and FTIR Spectrophotometers

Providing the utmost in sensitivity, accuracy and resolution for applications in materials characterization and science

- Photovoltaics
- Ceramics
- DNA film structures

PolymersCoatings

Paints

- Thin filmsInks
- Packaging materials
- Nanotechnology
- Click here for accurate, cost-effective laboratory solutions







Note: A simple image processing based fiducial auto-alignment method for sample registration

Wesley D. Robertson,¹ Lucas R. Porto,² Candice J. X. Ip,² Megan K. T. Nantel,² Friedjof Tellkamp,¹ Yinfei Lu,¹ and R. J. Dwayne Miller^{1,3,a)}

¹Max Planck Institute for the Structure and Dynamics of Matter, Hamburg 27761, Germany

²Department of Physics and Astronomy, University of British Columbia, Vancouver, British Columbia V6T 1Z4, Canada

(Received 9 July 2015; accepted 11 August 2015; published online 25 August 2015)

A simple method for the location and auto-alignment of sample fiducials for sample registration using widely available MATLAB/LabVIEW software is demonstrated. The method is robust, easily implemented, and applicable to a wide variety of experiment types for improved reproducibility and increased setup speed. The software uses image processing to locate and measure the diameter and center point of circular fiducials for distance self-calibration and iterative alignment and can be used with most imaging systems. The method is demonstrated to be fast and reliable in locating and aligning sample fiducials, provided here by a nanofabricated array, with accuracy within the optical resolution of the imaging system. The software was further demonstrated to register, load, and sample the dynamically wetted array. © 2015 AIP Publishing LLC. [http://dx.doi.org/10.1063/1.4929408]

Accurate and reproducible registration of a sample with an experimental probe (such as a laser or molecular beam) is a necessity for many types of experiments. Included among these are techniques that utilize nanofabricated structures for sample localization, such as self-localizing micro well arrays, 1,2 microfluidic "lab on a chip" sample sorting and mixing devices, 3 as well as high throughput electron and x-ray crystallography sorting arrays. 4 Sample registration is typically performed using fiducial markers which are manually selected as reference positions using precision translation stages, imaging microscopy, and tedious operator selection which can increase the experiment setup time and introduce reproducibility errors. Toward this end, numerous techniques have been developed to incorporate fiducials onto various sample types and sample holders. 5-8 More recently, image processing methods have been employed in developing sophisticated techniques to correlate machine vision with accurate and reproducible fiducial location and further to achieve subpixel image resolution enhancement for applications requiring extreme speed and precision.9,10

In this note, we address the need for a widely available and easily implemented method for sample registration by using an image processing algorithm (IPA) available from MAT-LAB in conjunction with LabVIEW for instrument control. The method can be implemented quickly in any laboratory with access to these software packages. The software uses IPA characterized circular fiducials as a length calibration and only requires the sample fiducial diameter be known to within less than a factor of ~1.5. The iterative method accounts for inaccuracies in IPA diameter detection and permits accurate location of multiple fiducials separated by distances larger than

the camera field of view. We demonstrate alignment to be limited by the resolution of the imaging system. The software is shown here to locate and align sample fiducials provided by a nanofabricated well array and further scan, dynamically wet, and laser ablate the individual wetted wells within their evaporation time, extending the functionality of the device.

The method was implemented using home designed Lab-VIEW software (Version 14, National Instruments) linked to MATLAB (MathWorks, Inc., Natick, MA, USA) which managed video and image processing from a 0.3 megapixel (60 fps) camera (BFLY-U3-20S4M-CS, Point Grey Research, Richmond, Canada). The video was collected using a long working distance (95 mm) microscope (QIOPTIQ, Waltham, USA) with an adjustable magnification and optical resolution range from 233 to 71 lines/mm. Mechanical translation of the sample was performed via slip-stick piezo stages (13 mm/s, SLC-2445, SmarAct, Oldenburg, Germany) with a closed loop nano-positioning sensor (1 nm) which was used to measure alignment reproducibility. The stages were controlled via LabVIEW with feedback from the image processing being performed in MATLAB. The system was demonstrated here for dynamic wetting and ablation of a self-localizing array (61×61) designed and nanofabricated on silica nitride coated fused silica (100 μ m $\pm 0.5 \mu$ m with a depth of 300 nm ± 20 nm). The array was wetted using a variation of the dragged drop method¹ and ablated with a focused picosecond laser (3 μ m) operating under desorption by impulsive vibrational excitation (DIVE) conditions. 11 The array provided fiducial structural precision greater than the resolution of the imaging system for direct testing. The accuracy of the IPA center point location was measured directly from high resolution images. The technique was tested with the imaging system at 0° and 35° from the sample normal.

The fiducial auto-alignment software presented here is detailed schematically in Fig. 1 and demonstrated with the

³Department of Chemistry and Physics, University of Toronto, Toronto, Ontario M5S 3H6, Canada

a)Author to whom correspondence should be addressed. Electronic mail: dwayne.miller@mpsd.mpg.de

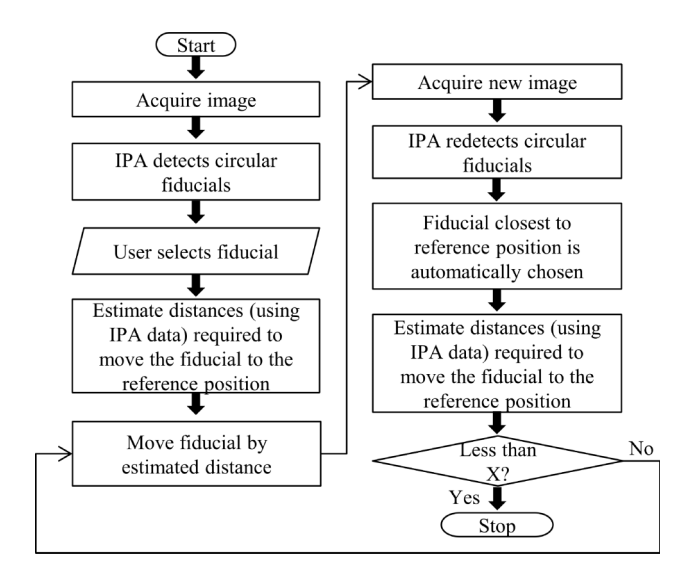


FIG. 1. A schematic representation of the image processing based autoalignment algorithm. The algorithm accurately locates the center position of circular fiducial markers on the sample by iteratively converging to their location using parameters obtained by the IPA.

nanofabricated fiducial array. Single images of the sample video were selected for each image processing iteration to optimize the overall speed. The readily available, Hough transform based ^{12,13} image processing algorithm (imfindcircles, MATLAB, Image Processing Toolbox 8.1) was chosen to identify the fiducial structure on the sample image. The IPA is optimized to locate circular structures with a preset radius range given an imperfect image input ^{14,15} and has been shown to be effective in detecting structures under a variety of imaging conditions. ^{16–18} The image processing constraints and parameters, radius minimum, radius maximum, selection sensitivity, and pixel edge selection threshold, are set within the LabVIEW user interface and can be adjusted for a variety of sample types, fiducial characteristics and imaging conditions.

The software was optimized for IPA fiducial detection considering the fiducial structural characteristics and imaging conditions (0° to the sample normal). Fiducials on the nanofabricated array were successfully located, as shown in Fig. 2(a). The center point location accuracy was measured to be 3.7 μ m, as described in Table I. Following successful image processing, a specific fiducial is selected by the user for alignment. The location of the center and the diameter of the selected fiducial, in camera pixel coordinates, is returned and used to estimate the distance between center of the fiducial mark and the user selected image reference position. The software uses the IPA measured and user input fiducial diameter to convert the camera pixel coordinates to a distance. The piezo stages are then translated to the estimated location to overlap the fiducial center with the reference position. Inaccuracies in IPA measured fiducial diameter commonly resulted in a distance estimate error of less than 10% given moderately optimized conditions. Following the first overlap iteration, the fiducial was moved to within 27 μ m of the reference point as shown in Fig. 2(b). A new image is then automatically selected from the video stream, image processed, and the distance between the centers of the new IPA located fiducials and the reference

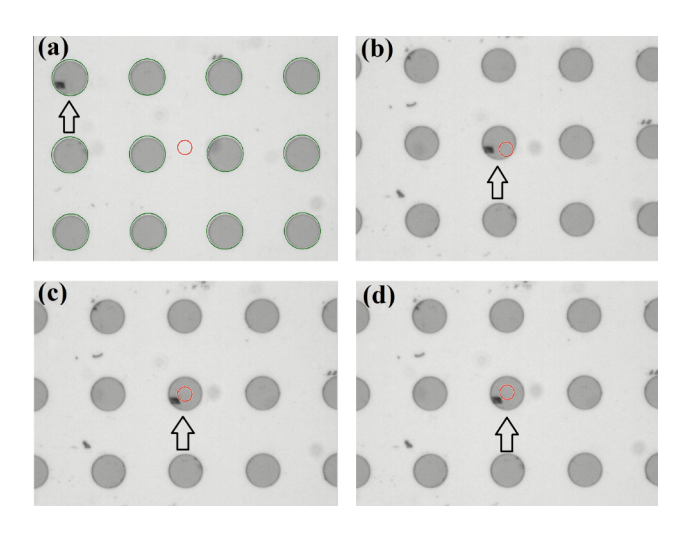


FIG. 2. Representative images of the IPA applied to the fiducial target, detected structure shown in green circles. Alignment iterations of the image reference position (red circle) with a nanofabricated fiducial, (a) before alignment initiation, (b) immediately following the first, (c) second, and (d) final auto-alignment iteration. IPA detection not shown in (b)–(d) for clarity.

position is re-estimated as described previously. The fiducial closest to the reference position is automatically selected. If the distance to the selected fiducial is greater than the user defined tolerance (5 μ m, \pm IPA error), the stages are moved again by the distance estimated to overlap the two points. This process is iterated until the distance estimated is less than the user defined accuracy, at which point the auto-alignment procedure is terminated and the position is stored. As shown in Fig. 2(d), subsequent iterations of the algorithm (n = 3, <5 s) aligned the fiducial to the reference point to within the tolerance value. The reproducibility of fiducial location and auto-alignment was measured to be 2.6 μ m as shown in Table I.

Inaccuracies in the IPA measured fiducial diameter and the known fiducial diameter contribute to pixel to distance conversion estimate errors. Further, it was observed that the IPA parameters and imaging conditions could be selected to result in IPA fiducial diameter error as large as 30%, though IPA diameter detection errors do not effect center point location of circular fiducials given they are concentric. Errors of this type are propagated to the distance estimate and increase the iterations necessary for alignment. Conditions were found that resulted in IPA detection that was not concentric to the fiducial and should be avoided to prevent alignment error. Successful alignment of the fiducial center with the reference position was achieved for input error as high as 1.9 times the known fiducial diameter (99 iterations, 130 s). Alignment was achieved within 15 s for the input diameters of 1.5 times the

TABLE I. Fiducial location accuracy and fiducial alignment reproducibility for the IPA software.

Viewing angle (deg)	Microscope resolution (μm)	IPA accuracy (μm) ^a	Alignment repeatability $(\mu m)^a$
0	5	3.7	2.6
35	12	7.4	1.8

 $^{{}^{}a}$ Root mean square, $N \ge 24$ determinations.

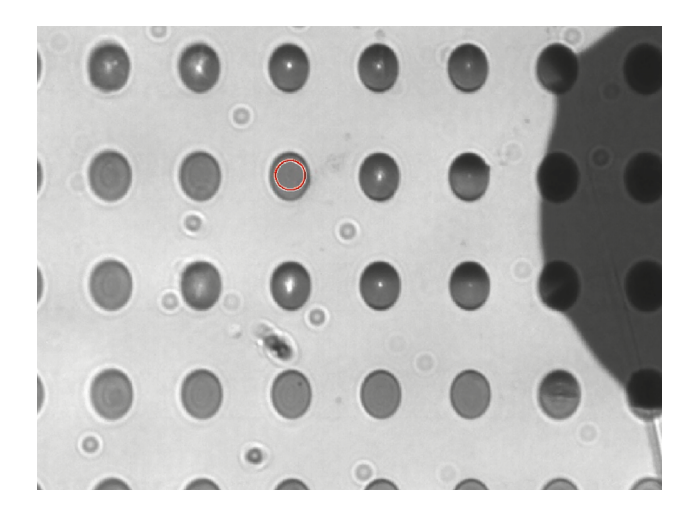


FIG. 3. Video demonstrating the implementation of the auto-alignment software for dynamic wetting and ablation (laser focus in red circle) of a nanofabricated well array. (Multimedia view) [URL: http://dx.doi.org/10.1063/1.4929408.1]

actual fiducial size. As expected, the alignment procedure was successful given smaller input values of the fiducial diameter and simply resulted in an increase in the number of iterations necessary for alignment. The distance calibration method is robust in that it can be used with any length scale fiducial, microscope magnification, and field of view allowing imaging adjustments without affecting the alignment method. Additional user features were implemented for ease of use, including stage speed, delay, and status as well as synchronized laser control. A script was also implemented to calculate the location of each well on the array relative to the auto-aligned fiducials and corrected for sample tilt.

The complete software is demonstrated under non-ideal imaging conditions (35° to the sample normal) for the dynamic aqueous wetting¹ and laser ablation of the nanofabricated array as shown in the videos in Fig. 3 (multimedia view). The software was used to select the laser focus as the image reference position and to perform the auto-alignment on three circular fiducial wells for sample registration. This sample registration procedure was successfully completed in less than 15 s. Enhanced alignment repeatability (1.8 μ m) was observed for 35° imaging, possibly due to the higher image contrast providing less variance in the IPA fitting of the fiducials. As demonstrated in Fig. 3 (multimedia view), the software successfully registered the sample and translated the sample wells to the laser focus for ablation before well evaporation (<1 s) following loading by dynamical wetting. Loaded wells are distinguished by their dark appearance. The maximum sampling frequency for the array was approximately 16 Hz (~1000 samples per minute) and was limited by the scanning speed of the piezo stages and the distance between the wells.

In conclusion, we have presented a robust, widely applicable, and readily implemented method for the accurate location and alignment of sample fiducials for sample registration. The method was successfully applied to a novel method of dynamically wetting and sampling nanofabricated wells within the well evaporation time. The method can readily be implemented for high throughput sampling of various types of nanofabricated sample arrays as well as easily modified for other applications including mass spectrometry, optical microscopy, laser etching, electron microscopy, nano-fluidics, and general pump-probe experiments. The software eliminates operator judgment error for fiducial alignment and increases the speed and reproducibility of alignment and sampling. Most importantly, the technique is easily implemented by most laboratories as it only requires MATLAB and LabVIEW or comparable software. The method can be significantly improved to overcome IPA tuning sensitivity and improve accuracy by implementing digital image filtering methods prior to IPA location and auto-alignment.¹⁰

This work was supported by the Max Planck Society. We would like to thank Sercan Keskin and Arash Zarrine-Afsar for assistance with nanofabrication and Cornelius Pieterse for his comments.

¹A. Zarrine-Afsar, C. Müller, F. O. Talbot, and R. J. D. Miller, Anal. Chem. **83**, 767 (2011).

²E. Miele, M. Malerba, M. Dipalo, E. Rondanina, A. Toma, and F. D. Angelis, Adv. Mater. 26, 4179 (2014).

³M. A. Khorshidi, P. K. P. Rajeswari, C. Wahlby, H. N. Joensson, and H. Andersson Svahn, Lab Chip 14, 931 (2014).

⁴A. Zarrine-Afsar, T. R. M. Barends, C. Muller, M. R. Fuchs, L. Lomb, I. Schlichting, and R. J. D. Miller, Acta Crystallogr., Sect. D: Biol. Crystallogr. **68**, 321 (2012).

⁵O. Rouvière, C. Reynolds, Y. Le, J. Lai, L. R. Roberts, J. P. Felmlee, and R. L. Ehman, J. Magn. Reson. Imaging **23**, 50 (2006).

⁶D. Bishop, I. Nikic, M. Brinkoetter, S. Knecht, S. Potz, M. Kerschensteiner, and T. Misgeld, Nat. Methods **8**, 568 (2011).

⁷K. Chughtai, L. Jiang, T. R. Greenwood, I. Klinkert, E. R. Amstalden van Hove, R. M. A. Heeren, and K. Glunde, Anal. Chem. **84**, 1817 (2012).

⁸T. R. McJunkin, T. L. Trowbridge, K. E. Wright, and J. R. Scott, Rev. Sci. Instrum. **85**, 023701 (2014).

⁹D. Weiliang and Y. James, Phys. Med. Biol. **54**, 555 (2009).

¹⁰Q. Wang, S. Nongliang, C. Maoyong, C. Anqing, and D. Fan, in 7th World Congress on Proceedings of Intelligent Control and Automation WCICA 2008, 2008.

¹¹K. Franjic and R. J. D. Miller, Phys. Chem. Chem. Phys. **12**, 5225 (2010).
¹²D. H. Ballard, Pattern Recognit. **13**, 111 (1981).

¹³J. Illingworth and J. Kittler, "Pattern analysis and machine intelligence," IEEE Trans. Pattern Anal. Mach. Intell. PAMI-9, 690 (1987).

¹⁴H. K. Yuen, J. Princen, J. Illingworth, and J. Kittler, Image Vision Comput. 8, 71 (1990).

¹⁵T. J. Atherton and D. J. Kerbyson, Image Vision Comput. 17, 795 (1999).

¹⁶Machine Vision, 3rd ed., edited by E. R. Davies (Morgan Kaufmann, Burlington, 2005).

¹⁷T. Kawaguchi, M. Rizon, and D. Hidaka, Electron. Commun. Jpn. 88, 29 (2005).

¹⁸Z. Qun, Y. Tat Soon, T. Hwee Siang, and L. Ying, IEEE Trans. Geosci. Remote Sens. 46, 291 (2008).